

What can lattice DFT teach us about real-space DFT?

Nahual Sobrino,¹ David Jacob,^{1,2} and Stefan Kurth*,^{1,2,3}

¹*Nano-Bio Spectroscopy Group and European Theoretical Spectroscopy Facility (ETSF),*

Departamento de Polímeros y Materiales Avanzados: Física, Química y Tecnología, Universidad del País Vasco UPV/EHU, Avenida Tolosa 72, E-20018 San Sebastián, Spain

²*IKERBASQUE, Basque Foundation for Science, Plaza Euskadi 5, E-48009 Bilbao, Spain*

³*Donostia International Physics Center (DIPC), Paseo Manuel de Lardizabal 4, E-20018 San Sebastián, Spain*

(* Corresponding author: stefan.kurth@ehu.es)

(Dated: 23 October 2023)

In this paper we establish a connection between density functional theory (DFT) for lattice models and common real-space DFT. We consider the lattice DFT description of a two-level model subject to generic interactions in Mermin's DFT formulation in the grand canonical ensemble at finite temperature. The case of only density-density and Hund's rule interaction studied in earlier work is shown to be equivalent to an exact-exchange description of DFT in the real-space picture. In addition, we also include the so-called pair-hopping interaction which can be treated analytically and, crucially, leads to non-integer occupations of the Kohn-Sham levels even in the limit of zero temperature. Treating the hydrogen molecule in a minimal basis is shown to be equivalent to our two-level lattice DFT model. By means of the fractional occupations of the KS orbitals (which, in this case, are identical to the many-body ones) we reproduce the results of full configuration interaction, even in the dissociation limit and without breaking the spin symmetry. Beyond the minimal basis, we embed our HOMO-LUMO model into a standard DFT calculation and, again, obtain results in overall good agreement with exact ones without the need of breaking the spin symmetry.

I. INTRODUCTION

Density Functional Theory (DFT) is in principle exact framework for solving the quantum many-body problem of interacting electrons.¹ The Kohn-Sham (KS) formulation of DFT allows to cast the problem into the particularly simple form of a system of effectively non-interacting electrons moving in a mean-field potential.² Owing to its computational efficiency, conceptual simplicity and in many cases high accuracy, KS-DFT has become one of the cornerstones of electronic structure theory and is now the standard tool for the description of electronic matter in computational condensed matter physics, material science and chemistry.³⁻⁵

One of the challenges for KS-DFT is the accurate description of so-called strongly correlated systems, for which the physics is dominated by the effects of strong electron-electron interactions. Important examples of these systems are transition-metal oxides, rare-earth compounds and transition-metal complexes. In these systems strong electronic correlations lead to very diverse phenomena such as the Mott metal-insulator transition, high-temperature superconductivity and spin-crossover behavior.⁶⁻⁹ One of the problems standard approximations to DFT struggle with is the proper description of multi-determinant, open-shell ground states within the KS framework which by construction is single-determinant.¹⁰⁻¹² To address this problem, various extensions to DFT have been proposed, such as the DFT+U method^{13,14} or the combination of DFT with dynamical mean-field theory (DMFT).¹⁵⁻¹⁹ However, these methods introduce additional parameters which can be hard to determine in an *ab initio* fashion and may still fail to properly describe a system in specific circumstances.^{20,21}

While DFT is usually formulated in real space and applied to real materials and molecules, it is also possible to formu-

late a DFT for lattice models, such as the Hubbard and Anderson impurity models.²²⁻²⁶ This allows to incorporate electron-electron interactions in a controlled way, and study their effect on the Hartree-exchange-correlation (Hxc) functional. Lattice DFT (LDFT) studies have for example revealed the ubiquitous presence of steps in the exact functionals.²⁷ It turns out that these steps are crucial for DFT to capture important aspects of strongly correlated systems by DFT, such as the Kondo plateau in the zero-bias conductance²⁸⁻³⁰ or the opening of a Mott gap.^{24,31} Furthermore, an extension of DFT which incorporates the current through an interacting system in addition to its density, called steady-state DFT or i-DFT, is capable of capturing strongly correlated phenomena both in the conductance and the many-body spectral function, such as Coulomb blockade, Kondo effect and the Mott metal-insulator transition.³²⁻³⁶ Again the proper description of these phenomena is typically linked to the presence of steps in the corresponding Hxc potentials.

An interesting question then is whether the insights obtained from LDFT can somehow be exploited to improve the performance of standard functionals of real-space DFT for molecules and materials in the presence of strong electronic correlations. The challenge lies in finding features of strong correlations that are generic enough to incorporate in approximate Hxc functionals in order to comply with the universal character of the true functional. A good testbed is the dissociation of the hydrogen (H₂) molecule, which despite its apparent simplicity presents a challenge for many electronic structure methods including DFT. Most approximate functionals encounter difficulties in accurately stretching H₂ without breaking the spin symmetry.¹⁰ At its heart H₂ dissociation is a strongly correlated problem: at large bond distances the many-body ground state acquires a pronounced multi-determinant character which poses a challenge to normal KS-DFT, as explained above.

In this work we first introduce the lattice DFT approach for a two-level system with different interactions (Sec. II) for which we present the Hxc energy and potential at $N = 2$ and functionals at low temperature. In Sec. III we propose a formal connection between lattice and real-space DFT and we identify the interactions in terms of KS orbitals. In Sec. IV, we apply this connection to the binding energy curve of the hydrogen molecule in minimal basis and beyond. Finally, we present our conclusions in Sec. V.

II. LATTICE DENSITY FUNCTIONAL THEORY FOR A TWO-LEVEL SYSTEM

First we review some results for the Hxc potentials for the particular interactions studied in Ref. 27. Then we will introduce an additional term to the interaction, the pair-hopping interaction, which at zero temperature, can be treated analytically within a density functional framework.

We consider a two-level system described by the Hamiltonian

$$\hat{H} = \sum_{i=1}^2 \varepsilon_i \hat{n}_i + \hat{W} \quad (1)$$

where ε_i is the single-particle energy of level i and $\hat{n}_i = \sum_{\sigma=\uparrow,\downarrow} \hat{n}_{i\sigma}$ with $\hat{n}_{i\sigma} = \hat{c}_{i\sigma}^\dagger \hat{c}_{i\sigma}$ and the $\hat{c}_{i\sigma}^\dagger$ ($\hat{c}_{i\sigma}$) are the creation (annihilation) operators for an electron with spin σ in level i . Finally, \hat{W} is the electron-electron interaction whose exact form will be specified below. We emphasize that the non-interacting part of the Hamiltonian of Eq. (1) is diagonal and that spin symmetry is not broken. In the following we work in the grand-canonical ensemble at finite temperature $T = \frac{1}{\beta}$ and chemical potential μ . As usual, expectation values of any operator \hat{O} are given by $O = \text{Tr}\{\hat{\rho}\hat{O}\}$ where the trace is over a complete set of states spanning the Fock space and the statistical operator is defined as

$$\hat{\rho} = \frac{1}{Z} \exp(-\beta(\hat{H} - \mu\hat{N})) . \quad (2)$$

Here, $Z = \text{Tr}\{\hat{\rho}\}$ is the partition function and $\hat{N} = \sum_{i=1}^2 \hat{n}_i$ is the operator for the total electron number.

Of course, since our model is so simple (and the corresponding Fock space small), it is straightforward to (numerically) exactly diagonalize the Hamiltonian \hat{H} for any conceivable interaction \hat{W} . However, a conceptually alternative approach for the calculation of the ‘‘densities’’ n_i is to use DFT in its incarnation of LDFT^{22,24}. Moreover, since we work in the grand-canonical ensemble, the proper DFT framework is given by Mermin’s finite temperature DFT³⁷. Therefore, we are looking for a non-interacting Hamiltonian, the Kohn-Sham (KS) Hamiltonian, of the form

$$\hat{H}_s = \sum_{i=1}^2 \varepsilon_i^s \hat{n}_i \quad (3)$$

with KS orbital energies ε_i^s which yields the same densities n_i as the interacting one. The KS orbital energies can be written

as $\varepsilon_i^s = \varepsilon_i + v_{\text{Hxc},i}$ with

$$v_{\text{Hxc},i}(n_1, n_2) = \frac{\partial \Omega_{\text{Hxc}}(n_1, n_2)}{\partial n_i} \quad (4)$$

where $\Omega_{\text{Hxc}}(n_1, n_2)$ is the Hxc contribution to the grand-canonical potential. Of course, the exact form of $\Omega_{\text{Hxc}}(n_1, n_2)$ depends on the interaction \hat{W} and, in the zero-temperature limit, it reduces to the Hxc energy contribution $E_{\text{Hxc}}(n_1, n_2)$ to the total ground state energy. For given, fixed single-particle energies ε_i of the interacting Hamiltonian (1), the self-consistent KS equations for our model then read

$$n_i = 2f(\varepsilon_i^s) = 2f(\varepsilon_i + v_{\text{Hxc},i}(n_1, n_2)) \quad (5)$$

where $f(x) = (1 + \exp(-\beta(x - \mu)))^{-1}$ is the Fermi function at inverse temperature β and chemical potential μ and the prefactor 2 is due to spin degeneracy. Since the r.h.s. of Eq. (5) depends on both densities, the two equations (5) for $i \in \{1, 2\}$ are coupled and have to be solved simultaneously.

In Ref. 27 we studied a two-level system with interactions of the form

$$\begin{aligned} \hat{W}_1 = & \sum_i U_i \hat{n}_{i\uparrow} \hat{n}_{i\downarrow} + U_{12} \hat{n}_1 \hat{n}_2 \\ & - J \left(\sum_{\sigma} \hat{n}_{1\sigma} \hat{n}_{2\sigma} + \hat{c}_{1\uparrow}^\dagger \hat{c}_{1\downarrow} \hat{c}_{2\downarrow}^\dagger \hat{c}_{2\uparrow} + \hat{c}_{1\downarrow}^\dagger \hat{c}_{1\uparrow} \hat{c}_{2\uparrow}^\dagger \hat{c}_{2\downarrow} \right) \end{aligned} \quad (6)$$

and found from reverse-engineering of exact results that the corresponding Hxc potentials in the zero-temperature limit have a structure dominated by step features which are intimately related to the famous derivative discontinuity of DFT.³⁸ Even in the zero-temperature limit, the exact form of the Hxc potential depends on the relative magnitude of the different interaction parameters. For parameters $U_1, U_2 \geq U_{12} \geq J$ we found that the Hxc potential for level i can be decomposed as

$$\begin{aligned} v_{\text{Hxc},i}(n_1, n_2) = & v_{\text{Hxc}}^{\text{CIM}}(U_{12} - J)[N] \\ & + v_{\text{Hxc}}^{\text{SSM}}(U_i - U_{12} + J)[n_i] + v_{\text{Hxc}}^{\text{Inter}}(J/2)[N] \end{aligned} \quad (7)$$

where

$$v_{\text{Hxc}}^{\text{CIM}}(U)[N] = \sum_{k=1}^3 U \theta(N - k) \quad (8)$$

is the Hxc potential of the Constant Interaction Model (CIM)^{26,39} with $N = n_1 + n_2$

$$v_{\text{Hxc}}^{\text{SSM}}(U)[n_i] = U \theta(n_i - 1) \quad (9)$$

is the Hxc potential of the Single Site Model (SSM)²⁸ and

$$v_{\text{Hxc}}^{\text{Inter}}(U)[N] = U \theta(N - 2) \quad (10)$$

is the interorbital term. Here we would also like to emphasize that in Eqs. (7) - (10) the function $\theta(x)$ should always be read as a function which in the zero-temperature limit approaches the Heaviside step function but in contrast to the Heaviside function remains continuous for any finite temperature T . By

integrating Eq. (7) one can then also derive the Hxc energy which reads

$$E_{\text{Hxc}}^{(1)}(n_1, n_2) = (U_{12} - J) \sum_{k=1}^3 (N-k) \theta(N-k) + \sum_{i=1}^2 (U_i - U_{12} + J)(n_i - 1) \theta(n_i - 1) + \frac{J}{2} (N-2) \theta(N-2) \quad (11)$$

Finally we would like to emphasize a peculiarity of the Hamiltonian (1) with interaction $\hat{W} = \hat{W}_1$ of Eq. (6): for this particular interaction, all eigenstates of \hat{H} are at the same time eigenstates of the operators \hat{n}_i with integer eigenvalues.

A. Including the pair-hopping interaction

Of course, the interaction of Eq. (6) is not the most general interaction possible in a two-level system. One generalization additionally includes the so-called pair hopping interaction (with strength P) which is written as

$$\hat{W}_2 = \hat{W}_1 - P \left(\hat{c}_{1\uparrow}^\dagger \hat{c}_{1\downarrow}^\dagger \hat{c}_{2\uparrow} \hat{c}_{2\downarrow} + \hat{c}_{2\uparrow}^\dagger \hat{c}_{2\downarrow}^\dagger \hat{c}_{1\uparrow} \hat{c}_{1\downarrow} \right). \quad (12)$$

We here restrict ourselves to the two-particle sector for which we choose the following 2-electron basis

$$\begin{aligned} |1\rangle &= \hat{c}_{1\uparrow}^\dagger \hat{c}_{1\downarrow}^\dagger |0\rangle & |4\rangle &= \hat{c}_{1\downarrow}^\dagger \hat{c}_{2\uparrow}^\dagger |0\rangle \\ |2\rangle &= \hat{c}_{1\uparrow}^\dagger \hat{c}_{2\uparrow}^\dagger |0\rangle & |5\rangle &= \hat{c}_{1\downarrow}^\dagger \hat{c}_{2\downarrow}^\dagger |0\rangle \\ |3\rangle &= \hat{c}_{1\uparrow}^\dagger \hat{c}_{2\downarrow}^\dagger |0\rangle & |6\rangle &= \hat{c}_{2\uparrow}^\dagger \hat{c}_{2\downarrow}^\dagger |0\rangle \end{aligned} \quad (13)$$

where $|0\rangle$ is the vacuum state. It is easy to check that states $|2\rangle$ and $|5\rangle$ are two degenerate eigenstates of the Hamiltonian (1) (with $\hat{W} = \hat{W}_2$) with eigenvalue $E_{2/5} = \varepsilon_1 + \varepsilon_2 + U_{12} - J$. From $|3\rangle$ and $|4\rangle$ we form the two eigenstates

$$|\tilde{3}\rangle = \frac{1}{\sqrt{2}}(|3\rangle - |4\rangle) \quad (14)$$

$$|\tilde{4}\rangle = \frac{1}{\sqrt{2}}(|3\rangle + |4\rangle) \quad (15)$$

with eigenvalues

$$\begin{aligned} E_{\tilde{3}} &= \varepsilon_1 + \varepsilon_2 + U_{12} + J \\ E_{\tilde{4}} &= \varepsilon_1 + \varepsilon_2 + U_{12} - J, \end{aligned} \quad (16)$$

i.e., $|\tilde{4}\rangle$ is degenerate with $|2\rangle$ and $|5\rangle$ (spin triplets). The remaining eigenstates $|\tilde{1}\rangle$ and $|\tilde{6}\rangle$ can be written as linear combination of states $|1\rangle$ and $|6\rangle$

$$|\tilde{1}\rangle = \cos \vartheta |1\rangle + \sin \vartheta |6\rangle \quad (17)$$

$$|\tilde{6}\rangle = -\sin \vartheta |1\rangle + \cos \vartheta |6\rangle \quad (18)$$

with some parameter ϑ to be specified and with eigenvalues

$$E_{\tilde{1}/\tilde{6}} = \varepsilon_1 + \varepsilon_2 + \frac{1}{2}(U_1 + U_2) \mp \frac{1}{2} \sqrt{(2\varepsilon_1 - 2\varepsilon_2 + U_1 - U_2)^2 + 4P^2}. \quad (19)$$

We note that out of all eigenstates, only states $|\tilde{1}\rangle$ and $|\tilde{6}\rangle$ can lead to a non-vanishing density difference $\Delta n = n_1 - n_2$. Without loss of generality (since ϑ hasn't been specified yet), we assume that out of the two eigenstates $|\tilde{1}\rangle$ and $|\tilde{6}\rangle$, $|\tilde{1}\rangle$ is the one with lower eigenvalue. The densities of this state can easily be computed as

$$\begin{aligned} n_1 &= \langle \tilde{1} | \hat{n}_1 | \tilde{1} \rangle = 2 \cos^2 \vartheta \\ n_2 &= \langle \tilde{1} | \hat{n}_2 | \tilde{1} \rangle = 2 \sin^2 \vartheta \end{aligned} \quad (20)$$

or

$$\Delta n = n_1 - n_2 = 2(\cos^2 \vartheta - \sin^2 \vartheta). \quad (21)$$

Eqs. (20) can then be used to express

$$\begin{aligned} \cos^2 \vartheta &= \frac{1}{2} \left(1 + \frac{\Delta n}{2} \right) \\ \sin^2 \vartheta &= \frac{1}{2} \left(1 - \frac{\Delta n}{2} \right) \end{aligned} \quad (22)$$

For our model, the Hohenberg-Kohn (HK) functional (which only depends on Δn) can be found from the constrained search approach as

$$F(\Delta n) = \min_{\Psi \rightarrow \Delta n} \langle \Psi | \hat{W}_2 | \Psi \rangle. \quad (23)$$

Since for given $\Delta n \neq 0$, the minimizing state $|\Psi_0\rangle$ must have the form (17), the HK functional can easily be evaluated as

$$\begin{aligned} F(\Delta n) &= \langle \tilde{1} | \hat{W}_2 | \tilde{1} \rangle \\ &= \frac{U_1}{2} \left(1 + \frac{\Delta n}{2} \right) + \frac{U_2}{2} \left(1 - \frac{\Delta n}{2} \right) - P \sqrt{1 - \frac{(\Delta n)^2}{4}} \end{aligned} \quad (24)$$

where the minus sign has to be chosen for the last (square root) term for the functional to be minimal for a given Δn . For $\Delta n = 0$, $F(\Delta n)$ of Eq. (24) coincides with the HK functional if the interaction parameters are such that $(U_1 + U_2)/2 - P < U_{12} - J$. For $(U_1 + U_2)/2 - P = U_{12} - J$ the states $|\tilde{1}\rangle$ and $|\tilde{4}\rangle$ become degenerate ground states (at $\Delta n = 0$) while for $(U_1 + U_2)/2 - P > U_{12} - J$ the state $|\tilde{4}\rangle$ becomes the unique ground state. It is important to note that the states $|\tilde{1}\rangle$ and $|\tilde{4}\rangle$ have a very different character. While the former is a spin singlet formed as linear combination of Slater determinants each with a single orbital occupied by two electrons, the latter is a triplet formed as linear combination of Slater determinants each with two different orbitals occupied by a single electron. It is exactly for this reason that in the limit $J = P = 0$, Eq. (24) reduces to $(U_1 + U_2)/2$ (for $\Delta n = 0$) while at the same densities the proper HK functional for $(U_1 + U_2)/2 > U_{12}$ (which follows from integrating Eq. (13) of Ref. 27) gives the value U_{12} .

Since in our model there is no kinetic energy contribution (neither in the interacting nor the non-interacting case), the functional for the Hxc energy is identical to the HK functional

$$E_{\text{Hxc}}(\Delta n) = F(\Delta n) \quad (25)$$

and the Hxc potentials are

$$\begin{aligned} v_{\text{Hxc},1}(\Delta n) &= \frac{U_1 - U_2}{4} + \frac{P\Delta n}{4\sqrt{1 - \frac{(\Delta n)^2}{4}}} \\ v_{\text{Hxc},2}(\Delta n) &= -\frac{U_1 - U_2}{4} - \frac{P\Delta n}{4\sqrt{1 - \frac{(\Delta n)^2}{4}}} \end{aligned} \quad (26)$$

or

$$\begin{aligned} \Delta v_{\text{Hxc}}(\Delta n) &= v_{\text{Hxc},1}(\Delta n) - v_{\text{Hxc},2}(\Delta n) \\ &= \frac{U_1 - U_2}{2} + \frac{P\Delta n}{2\sqrt{1 - \frac{(\Delta n)^2}{4}}} \end{aligned} \quad (27)$$

Knowing the HK functional $F(\Delta n)$, we can for given values of the single-particle parameters (on-site energies) $\varepsilon_1 = \frac{\Delta\varepsilon_0}{2}$ and $\varepsilon_2 = -\frac{\Delta\varepsilon_0}{2}$ find the corresponding ground state density Δn_0 by minimizing the HK total energy functional

$$E_{\Delta\varepsilon_0}(\Delta n) = \frac{\Delta\varepsilon_0}{2}\Delta n + F(\Delta n), \quad (28)$$

i.e., we solve

$$\begin{aligned} \left. \frac{\partial E_{\Delta\varepsilon_0}(\Delta n)}{\partial \Delta n} \right|_{\Delta n = \Delta n_0} &= 0 \\ &= \Delta\varepsilon_0 + \frac{U_1 - U_2}{4} + \frac{P}{4} \frac{\Delta n_0}{\sqrt{1 - \frac{(\Delta n_0)^2}{4}}}. \end{aligned} \quad (29)$$

This can be rearranged for Δn_0 and gives

$$\Delta n_0 = -\frac{2(2\Delta\varepsilon_0 + U_1 - U_2)}{\sqrt{(2\Delta\varepsilon_0 + U_1 - U_2)^2 + 4P^2}} \quad (30)$$

where the minus sign was chosen for the physical reason that we should have $\Delta n_0 \rightarrow 2$ for $\Delta\varepsilon_0 \rightarrow -\infty$. Reinserting this density into the HK energy functional (28), one can easily confirm that one obtains the ground state energy E_1 of Eq. (19).

Above we have computed the ground state density Δn_0 directly from the HK variational principle. The same result should, of course, also be obtained by self-consistent solution of the KS equations (5). For given single-particle parameters ε_i , these equations can be conveniently rewritten as

$$\Delta n = 2[f(\varepsilon_1 + v_{\text{Hxc},1}(\Delta n)) - f(\varepsilon_2 + v_{\text{Hxc},2}(\Delta n))] \quad (31)$$

and the solution of this equation has to coincide with the ground state density of Eq. (30) which we have confirmed numerically. In the upper panel of Fig. 1 we show the density imbalance Δn as function of $\Delta\varepsilon = \varepsilon_1 - \varepsilon_2$ for different values of the pair hopping parameter P and different temperatures. The other parameters are $U_1 = U_2 = U_{12} = 1.0$ and $J = P$ and where chosen to ensure that the ground state has the form of Eq. (17) for any $\Delta\varepsilon$. As expected, the stronger the pair-hopping interaction, the more the step in Δn at $\Delta n = 0$ is smoothed. We have solved both the many-body problem as well as the self-consistent solution of the corresponding KS

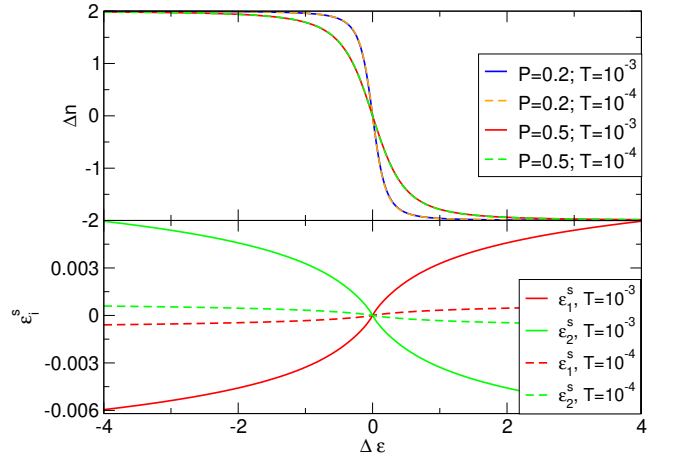


FIG. 1. Upper panel: Density imbalance $\Delta n = n_1 - n_2$ versus single particle energy difference $\Delta\varepsilon = \varepsilon_1 - \varepsilon_2$ for the model described by the Hamiltonian (1) with interaction \hat{W}_2 of Eq. (12) for different values of the pair-hopping interaction P and different temperatures T . The other parameters are $U_1 = U_2 = U_{12} = 1.0$ and $J = P$. Lower panel: KS eigenvalues $\varepsilon_i^s = \varepsilon_i + v_{\text{Hxc},i}$ at self-consistency for $P = J = 0.5$ and two different temperatures T . The other parameters are $U_1 = U_2 = U_{12} = 1.0$. All energies given in units of U_1 .

system and both solutions are identical on the scale of the figure (not shown). Moreover, we have computed Δn for two different, small temperatures T and found no appreciable difference in the corresponding density imbalances. However, we would like to draw attention to the particular way in which the KS system achieves the same density as the interacting one. We first note that the Fermi functions in the zero temperature limit approaches a step function and naively, Eq. (31) seems to suggest that its solution can only be ± 2 which is clearly not the case for arbitrary values of $\Delta\varepsilon$. Therefore, the Hxc potential must lead to total KS energies to be close to the chemical potential, i.e., the step region of the Fermi functions. This is confirmed by looking at the lower panel of Fig. 1 where we show the self-consistent KS eigenvalues for the parameters of the upper panel with $P = 0.5$ at two small temperatures. While the density already is basically converged at $T = 10^{-3}$, the KS eigenvalues are not. In fact, in the $T \rightarrow 0$ limit the KS eigenvalues will converge to the chemical potential μ (here taken to be zero) because they have to reproduce the densities. This can only be achieved by moving the KS eigenvalues onto the step of the Fermi function whose width is of the order of T . Even in this limit, however, the upper and lower KS eigenvalues have to converge to slightly different values in order to give a finite density imbalance Δn . This highlights the importance of working at small but finite temperature for which the Fermi functions exhibit a step but are not mathematically discontinuous. This is somewhat related to findings in previous works^{28,40} where it was found that Hxc potentials which exhibit step structures typically lead to a pinning of KS energy levels to the Fermi energy for a range of single-particle energies.

III. ESTABLISHING A CONNECTION BETWEEN LATTICE DFT AND REAL-SPACE DFT

In the present Section and based on the results of the previous Section, we will establish a connection between lattice DFT and the usual DFT formulation in real space. The combination of standard DFT with advanced many-body treatments of lattice models has a long tradition, possibly starting with what is known as DFT+U method¹³. A more recent approach combines dynamical mean-field theory (DMFT) with DFT^{15,17,19}. In a somewhat different line, a direct transfer of ideas from lattice DFT to standard quantum chemical methods has been suggested recently⁴¹. Here we suggest an alternative connection between lattice DFT and real-space DFT based on our results for the two-level system described in Sec. II.

In Mermin's version of finite-temperature DFT³⁷, the electronic density (in real space) in thermal equilibrium for an interacting many-electron system subject to an electrostatic potential $v_0(\mathbf{r})$ is determined by self-consistent solution of the KS equation

$$\left(-\frac{\nabla^2}{2} + v_0(\mathbf{r}) + v_{\text{Hxc}}[\rho](\mathbf{r})\right) \varphi_{i\sigma}(\mathbf{r}) = \varepsilon_{i\sigma}^s \varphi_{i\sigma}(\mathbf{r}) \quad (32)$$

with the KS orbitals $\varphi_{i\sigma}$ and the KS energy eigenvalues $\varepsilon_{i\sigma}^s$. The electronic density is given by

$$\rho(\mathbf{r}) = \sum_{i\sigma} n_{i\sigma} |\varphi_{i\sigma}(\mathbf{r})|^2 \quad (33)$$

where the occupation of the KS orbital $\varphi_{i\sigma}$ is given by $n_{i\sigma} = f(\varepsilon_{i\sigma}^s)$. In Eq. (32), the Hxc potential is given as functional derivative of the Hxc contribution Ω_{Hxc} to the grand canonical potential, i.e.,

$$v_{\text{Hxc}}[\rho](\mathbf{r}) = \frac{\Omega_{\text{Hxc}}[\rho]}{\delta\rho(\mathbf{r})} \quad (34)$$

which, of course, has to be approximated in practice.

In Sec. II we have found the Hxc energy E_{Hxc} (i.e., the zero-temperature limit of Ω_{Hxc}) for the two-level system as function of the occupation numbers n_i and the interaction parameters U_i , U_{12} , J , and P . In order to make a connection between these lattice DFT results and real-space DFT, we now propose to interpret the occupation numbers as $n_i = \sum_{\sigma} n_{i\sigma} = \sum_{\sigma} f(\varepsilon_{i\sigma}^s)$ and the interaction parameters as two-electron Coulomb integrals with respect to the KS orbitals. We define a general two-electron integral as

$$(i\sigma j\sigma | k\sigma' l\sigma') = \int d^3r \int d^3r' \frac{\varphi_{i\sigma}^*(\mathbf{r}) \varphi_{j\sigma}(\mathbf{r}) \varphi_{k\sigma'}^*(\mathbf{r}') \varphi_{l\sigma'}(\mathbf{r}')}{|\mathbf{r} - \mathbf{r}'|} \quad (35)$$

Then the interaction parameters can be identified in terms of these two-electron integrals as

$$\begin{aligned} U_i &= (i\sigma i\sigma | i\bar{\sigma} i\bar{\sigma}) & J &= (1\sigma 2\sigma | 2\sigma 1\sigma) \\ U_{12} &= (1\sigma 1\sigma | 2\sigma 2\sigma) & P &= (1\sigma 2\bar{\sigma} | 1\bar{\sigma} 2\sigma) \end{aligned} \quad (36)$$

where $\bar{\sigma} = \downarrow (\uparrow)$ for $\sigma = \uparrow (\downarrow)$. We note that for real and spin-independent KS orbitals we have $J = P$. With this interpretation, the interaction parameters formally become functionals

of the KS orbitals and the occupation numbers functionals of the KS energy eigenvalues. In the context of DFT, functionals depending on KS orbitals and KS eigenvalues are *implicit* functionals of the density and it is well known that the corresponding (Hxc) potentials (i.e., functional derivatives with respect to the density) can be computed with the Optimized Effective Potential (OEP) formalism⁴²⁻⁴⁴.

We now take a look at what our interpretation of the lattice DFT functionals in terms of real-space KS orbitals and occupation numbers implies for the specific example of $E_{\text{Hxc}}^{(1)}$ given by Eq. (11). We will not consider general values for n_1 and n_2 but instead focus on those points where both occupation numbers are integer. For $n_1 = n_2 = 0$ as well as for $n_1 = 1$, $n_2 = 0$ and $n_1 = 0$, $n_2 = 1$ we see that $E_{\text{Hxc}}^{(1)}$ vanishes, i.e., $E_{\text{Hxc}}^{(1)}$ is self-interaction free for one electron. For $n_1 = 2$ and $n_2 = 0$ we find $E_{\text{Hxc}}^{(1)}(n_1 = 2, n_2 = 0) = U_1$ which can be written as

$$E_{\text{Hxc}}^{(1)}(n_1 = 2, n_2 = 0) = \frac{1}{4} \int d^3r \int d^3r' \frac{\rho(\mathbf{r})\rho(\mathbf{r}')}{|\mathbf{r} - \mathbf{r}'|} \quad (37)$$

where we assumed spin-independent KS orbitals such that the density becomes $\rho(\mathbf{r}) = 2|\varphi_{1\sigma}(\mathbf{r})|^2$. The same result (in terms of the density) is obtained for $n_1 = 0$, $n_2 = 2$. For full occupation of the two-level system, $n_1 = 2$, $n_2 = 2$, we obtain $E_{\text{Hxc}}^{(1)}(n_1 = 2, n_2 = 2) = 4U_{12} + U_1 + U_2 - 2J$ which can be written as

$$\begin{aligned} E_{\text{Hxc}}^{(1)}(n_1 = 2, n_2 = 2) &= \frac{1}{2} \int d^3r \int d^3r' \frac{\rho(\mathbf{r})\rho(\mathbf{r}')}{|\mathbf{r} - \mathbf{r}'|} \\ &- \frac{1}{2} \sum_{\sigma} \sum_{i,j=1}^2 \int d^3r \int d^3r' \frac{\varphi_{i\sigma}^*(\mathbf{r}) \varphi_{j\sigma}(\mathbf{r}) \varphi_{2\sigma}^*(\mathbf{r}') \varphi_{1\sigma}(\mathbf{r}')}{|\mathbf{r} - \mathbf{r}'|} \end{aligned} \quad (38)$$

We recognize that both Eq. (37) and (38) are nothing but the Hartree plus the exact exchange energy of standard DFT. In fact, also for the other integer occupations the functional of Eq. (11) can with our interpretation (lattice densities identified as occupations of KS orbitals and interaction parameters defined in terms of KS orbitals) be identified as the Hartree plus exact exchange functionals. However, for occupations $n_1 = 2$, $n_2 = 1$ and $n_1 = 1$, $n_2 = 2$ as well as for $n_1 = n_2 = 1$ this identification requires the use of the proper definition of the Hartree plus exact exchange energy of ensemble DFT derived in Refs. 45 and 46. Based on the recovery of the Hartree plus exact exchange energy for integer occupations, we may infer that the energy functional of Eq. (11) is actually the proper generalization of this functional for any non-integer occupation $0 \leq n_i \leq 2$. Furthermore, from the recovery of a known functional from Eq. (11), we also gain confidence that the functional of Eq. (25) with our interpretation is a reasonable approximation to the exact Hxc functional of a two-level system. This will be borne out in the next Section where we apply the functional (25) to the description of the H_2 molecule.

IV. APPLICATION TO THE HYDROGEN MOLECULE

In the present Section we describe an application of the formalism presented in Sec. II to the hydrogen molecule. We

start with the problem treated with a minimal basis set before investigating larger basis sets.

A. Minimal basis set

In the minimal basis for the hydrogen molecule (H_2), for each atom we have only one single s -type basis function. Let $g(\mathbf{r}) (= g(-\mathbf{r}))$ be such an s -type normalized (real) basis function localized at the origin $\mathbf{r}_0 = \mathbf{0}$. If we take the hydrogen atoms to be located at $\pm \mathbf{R}/2$, from the localized basis functions $g_{1/2}(\mathbf{r}) = g(\mathbf{r} \pm \mathbf{R}/2)$ we can construct two normalized and orthogonal (spin) orbitals, one bonding and one anti-bonding, which take the form

$$\begin{aligned}\varphi_1(\mathbf{r}) &= \varphi_{1\sigma}(\mathbf{r}) = \frac{1}{\sqrt{2(1+S)}} (g_1(\mathbf{r}) + g_2(\mathbf{r})) \\ \varphi_2(\mathbf{r}) &= \varphi_{2\sigma}(\mathbf{r}) = \frac{1}{\sqrt{2(1-S)}} (g_1(\mathbf{r}) - g_2(\mathbf{r}))\end{aligned}\quad (39)$$

where

$$S = \int d^3r g_1(\mathbf{r})g_2(\mathbf{r}) \quad (40)$$

is the overlap integral of the two localized basis functions. We note that by construction the $\varphi_k(\mathbf{r})$ are eigenfunctions of the parity operator, i.e., they satisfy the symmetry relations

$$\varphi_1(-\mathbf{r}) = \varphi_1(\mathbf{r}) \quad \varphi_2(-\mathbf{r}) = -\varphi_2(\mathbf{r}) \quad (41)$$

When written in terms of field operators, the Hamiltonian of the hydrogen molecule is given by

$$\begin{aligned}\hat{H}_{H_2} &= \sum_{\sigma} \int d^3r \hat{\psi}_{\sigma}^{\dagger}(\mathbf{r}) \hat{h}_0(\mathbf{r}) \hat{\psi}_{\sigma}(\mathbf{r}) + E_{\text{nuc}}(R) \\ &+ \frac{1}{2} \sum_{\sigma, \sigma'} \int d^3r \int d^3r' \hat{\psi}_{\sigma}^{\dagger}(\mathbf{r}) \hat{\psi}_{\sigma'}^{\dagger}(\mathbf{r}') \frac{1}{|\mathbf{r} - \mathbf{r}'|} \hat{\psi}_{\sigma'}(\mathbf{r}') \hat{\psi}_{\sigma}(\mathbf{r})\end{aligned}\quad (42)$$

with the single-particle Hamiltonian

$$\hat{h}_0(\mathbf{r}) = -\frac{\nabla^2}{2} + v(\mathbf{r}) \quad (43)$$

where $v(\mathbf{r})$ is the attractive potential due to the protons

$$v(\mathbf{r}) = -\frac{1}{|\mathbf{r} - \mathbf{R}/2|} - \frac{1}{|\mathbf{r} + \mathbf{R}/2|}, \quad (44)$$

and the nuclear electrostatic repulsion energy $E_{\text{nuc}}(R) = 1/R$ with $R = |\mathbf{R}|$.

In the minimal basis, the field operators can be written as

$$\hat{\psi}_{\sigma}^{\dagger}(\mathbf{r}) = \sum_{i=1}^2 \varphi_{i\sigma}^*(\mathbf{r}) \hat{c}_{i\sigma}^{\dagger} \quad (45)$$

where the $\hat{c}_{i\sigma}^{\dagger}$ are the creation operators for an electron in orbital $\varphi_{i\sigma}$. When inserted into Eq. (42) the Hamiltonian of the

H_2 molecule in the minimal basis (mb) takes the form

$$\begin{aligned}\hat{H}_{H_2}^{\text{mb}} &= \sum_{i=1}^2 \varepsilon_i \hat{n}_i + E_{\text{nuc}}(R) \\ &+ \frac{1}{2} \sum_{\sigma, \sigma'} \sum_{i,j,k,l=1}^2 (i\sigma j\sigma' | k\sigma' l\sigma) \hat{c}_{i\sigma}^{\dagger} \hat{c}_{j\sigma'}^{\dagger} \hat{c}_{k\sigma'} \hat{c}_{l\sigma}\end{aligned}\quad (46)$$

where the single-particle energies are given by

$$\varepsilon_i = \langle i\sigma | \hat{h}_0(\mathbf{r}) | i\sigma \rangle \quad (47)$$

and the off-diagonal matrix elements of $\hat{h}_0(\mathbf{r})$ vanish due to the symmetry $\hat{h}_0(-\mathbf{r}) = \hat{h}_0(\mathbf{r})$ together with the symmetry (41) of the basis functions, i.e.,

$$\langle i\sigma | \hat{h}_0(\mathbf{r}) | j\sigma' \rangle = \delta_{\sigma\sigma'} \delta_{ij} \int d^3r \varphi_{i\sigma}^*(\mathbf{r}) \hat{h}_0(\mathbf{r}) \varphi_{j\sigma}(\mathbf{r}) = \delta_{\sigma\sigma'} \delta_{ij} \varepsilon_i. \quad (48)$$

Again, due to the symmetry (41) of the basis functions, it is easy to show that all those two-electron integrals vanish for which three of the four indices $\{i, j, k, l\}$ are equal and the Hamiltonian for H_2 in the minimal basis becomes

$$\hat{H}_{H_2}^{\text{mb}} = \sum_{i=1}^2 \varepsilon_i \hat{n}_i + \hat{W}_2 + E_{\text{nuc}}(R). \quad (49)$$

Since this Hamiltonian now has exactly the form of the one studied in the Sec. II (plus the additive nuclear repulsion energy), the total energy functional of H_2 takes the form

$$E_{H_2}(\Delta n) = \sum_{i=1}^2 \varepsilon_i n_i + F(\Delta n) + E_{\text{nuc}}(R) \quad (50)$$

with the HK functional of Eq. (28). The direct minimization for Δn as well as the solution of the corresponding KS equation (31) proceed as described in Sec. II and the resulting difference in occupation numbers is given by Eq. (30). Note that here we are only minimizing the occupation number difference while the orbitals of Eq. (39) remain fixed.

We have mapped out the binding energy curve for the H_2 molecule in minimal basis with the open source PySCF code⁴⁷. We calculated, for each internuclear distance R , the interaction parameters U_i and P as well as the corresponding matrix elements (47) which enter in the evaluation of the occupation numbers (Eq. (30)). The total energy was then computed by adding the internuclear repulsion to the total energy functional (28). In the minimal basis, our approach becomes exact and therefore equivalent to full configuration interaction (FCI) which can be confirmed analytically⁴⁸. In Fig. 2 we show the binding energy curves from our approach and compare with standard spin-restricted Hartree-Fock (HF) as well as DFT calculations using the LDA and PBE functionals⁴⁹. As expected, our approach recovers the full CI results while both spin-restricted HF and standard DFT, as is well-known, do not recover the correct large separation limit (see, however, the partition DFT of Refs. 50 and 51 which also captures dissociation without breaking the spin symmetry). The reason why our approach does indeed recover this limit simply

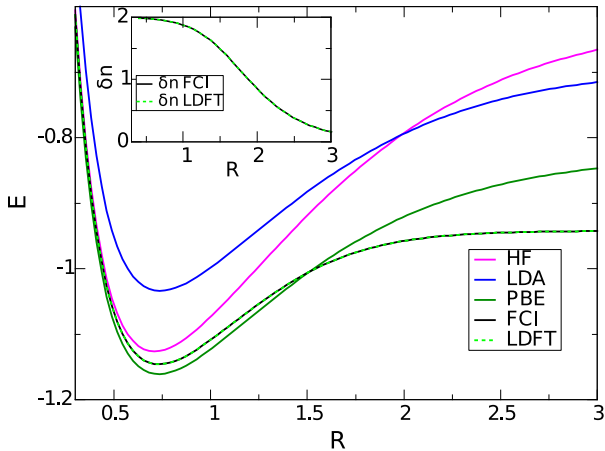


FIG. 2. Binding energy of the hydrogen molecule in minimal basis as function of the internuclear separation R for various spin-restricted approaches: Hartree-Fock (HF) as well as the DFT approaches using the LDA and PBE functionals and our functional (LDFT). The full CI result is given as reference. In the inset we show the occupation number difference in full CI as function of R which is identical to our LDFT result. All quantities given in atomic units.

lies in the fact that both the ground-state Slater determinant as well as the doubly excited Slater determinant contribute, i.e., the occupation numbers n_1 and n_2 are not strictly integer. In the context of our DFT approach this is possible because we are working with the equilibrium grand-canonical *ensemble* of non-interacting KS wavefunctions and not just with the KS ground state wavefunction.

B. Beyond the minimal basis

We have also evaluated the binding energy curves of the hydrogen molecule within our approach but using a larger basis. To this end, we performed self-consistent HF, LDA, and PBE calculations with the larger cc-pvtz basis⁴⁷. From the resulting lowest-lying molecular KS orbitals, the HOMO orbital $\phi_H(\mathbf{r}) = \phi_{1\sigma}(\mathbf{r})$ and orbital energy $\varepsilon_H = \varepsilon_1$ as well as the LUMO orbital $\phi_L(\mathbf{r}) = \phi_{2\sigma}(\mathbf{r})$ with orbital energy $\varepsilon_L = \varepsilon_2$ we evaluate both the single-particle matrix elements of Eq. (47) as well as all the interaction parameters. Note that the orbital energies ε_i are *not* KS energy eigenvalues but the expectation values of the *core* Hamiltonian in the KS orbitals, as defined by Eq. (47). Once these parameters are determined, we evaluate the total energy according to Eq. (50), i.e., we find the orbital occupations n_i which minimize the total energy according to our two-level model while keeping the orbitals fixed.

In the left panel of Fig. 3 we show the binding energy curves obtained in our approach from the three different sets of self-consistent molecular (spin-restricted) orbitals obtained with the three different functionals in comparison to the corresponding standard spin-restricted and full CI results. As a common theme, for the three sets of orbitals the large separation limit is captured correctly with our approach unlike

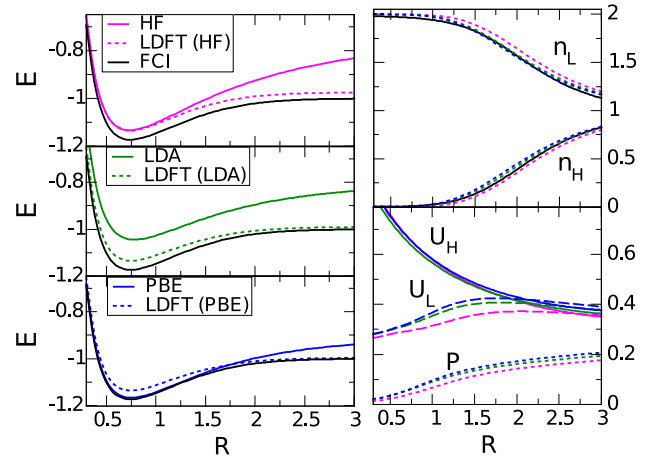


FIG. 3. Left panel: Binding energy of the hydrogen molecule in cc-pvtz basis as function of internuclear separation R using HF, LDA, and PBE (spin-restricted) self-consistent orbitals to evaluate the energy with our approach in comparison to full CI results. Upper right panel: occupation numbers of the HOMO and LUMO KS orbitals as function of R computed from different self-consistent orbitals. Lower right panel: interaction parameters as function of R from different orbitals. All quantities given in atomic units.

for the spin-restricted self-consistent calculations. The closest results to the full CI reference in this limit is achieved with PBE, followed by LDA and HF. Around the equilibrium bond distance the three sets of orbitals lead to similar results, very close to self-consistent HF. LDA orbitals give significantly improved total energies as compared to self-consistent LDA results, while PBE orbitals give slightly worse energies than self-consistent PBE ones.

In the upper right panel of Fig. 3 we compare orbital occupations from our approach with the three sets of orbitals. They all follow reasonably well the exact reference results with HF performing slightly worse. The interaction parameters (lower right panel of Fig. 3) from the three sets of orbitals are reasonably similar among each other, again with HF showing more pronounced differences to the DFT results, especially for the interaction parameter U_L corresponding to the LUMO orbital.

As discussed above, the results of the present Section for our approach were not computed self-consistently but with orbitals obtained either from HF or other DFT functionals. In principle our two-level functional can be read as an orbital-dependent functional which requires the OEP method for calculation of the corresponding self-consistent potential which, however, is beyond the scope of the present work.

V. SUMMARY AND CONCLUSIONS

The present work was motivated by earlier work²⁷ on a simple model of a double quantum dot on a lattice subject to different types of electron-electron interactions. We aimed at finding possible connections between lattice DFT (here in the framework of Mermin's finite-temperature version of DFT

in the grand-canonical ensemble³⁷) and real-space DFT. This connection could be found if the interaction parameters of the lattice DFT model are read as two-electron Coulomb integrals with respect to the KS orbitals of real-space DFT and the lattice “densities” are interpreted as the occupation numbers of these KS orbitals. For the interactions studied in Ref. 27 we found that, for integer occupation of the orbitals, this interpretation leads to a recovery of the exact-exchange energy functional.

We also studied an additional term to the interaction in the lattice model, the pair-hopping interaction, for which we found the analytical form of the exact HK energy functional. As a crucial difference to the previously studied interactions, we found that the pair-hopping term leads to non-integer occupations of the KS orbitals even in the limit of zero temperature. Another connection to real-space DFT could be established by showing that the Hamiltonian of the hydrogen molecule (H_2), when treated in a minimal basis of localized basis functions, has exactly the form of our lattice model with the pair-hopping term included. Knowing the exact HK energy functional (and therefore also the exact Hxc energy functional) for this model, the binding energy curve of H_2 was found to coincide with the full CI one in the minimal basis for *all* internuclear distances and without the need of breaking spin symmetry. This is achieved by both the KS ground state and the doubly excited KS determinant having finite weight in the KS ensemble (in the zero-temperature limit) which is equivalent to saying that both HOMO and LUMO KS orbitals have non-integer occupation in this ensemble. Finally, we suggested a post-SCF evaluation of our energy functional for larger basis sets allowing to recover the correct large-separation limit without spin symmetry breaking. This latter approach still requires a self-consistent treatment, e.g., within the OEP approach, which will be the subject of future work.

ACKNOWLEDGMENTS

We acknowledge financial support through Grant PID2020-112811GB-I00 funded by MCIN/AEI/10.13039/501100011033 as well as by grant IT1453-22 “Grupos Consolidados UPV/EHU del Gobierno Vasco”.

¹P. Hohenberg and W. Kohn, Phys. Rev. **136**, B864 (1964).

²W. Kohn and L. Sham, Phys. Rev. **140**, A1133 (1965).

³R.G. Parr and W. Yang, *Density-Functional Theory of Atoms and Molecules* (Oxford University Press, New York, 1989).

⁴R.M. Dreizler and E.K.U. Gross, *Density Functional Theory* (Springer, Berlin, 1990).

⁵K. Burke, J. Chem. Phys. **136**, 150901 (2012).

⁶M. Imada, A. Fujimori, and Y. Tokura, Rev. Mod. Phys. **70**, 1039 (1998).

⁷P. A. Lee, N. Nagaosa, and X.-G. Wen, Rev. Mod. Phys. **78**, 17 (2006).

⁸P. Gütllich, A. B. Gaspar, and Y. Garcia, Beilstein J. Org. Chem. **9**, 342 (2013).

⁹C. Ahn, A. Cavalleri, A. Georges, S. Ismail-Beigi, A. J. Millis, and J.-M. Triscone, Nat. Mater. **20**, 1462 (2021).

¹⁰A. J. Cohen, P. Mori-Sánchez, and W. Yang, Chem. Rev. **112**, 289 (2012).

¹¹N. Q. Su and X. Xu, Annu. Rev. Phys. Chem. **68**, 155 (2017).

¹²J. P. Perdew, A. Ruzsinszky, J. Sun, N. K. Nepal, and A. D. Kaplan, Proc. Natl. Acad. Sci. USA **118**, e2017850118 (2021).

¹³V. I. Anisimov, J. Zaanen, and O. K. Andersen, Phys. Rev. B **44**, 943 (1991).

¹⁴L. Wang, T. Maxisch, and G. Ceder, Phys. Rev. B **73**, 195107 (2006).

¹⁵G. Kotliar, S. Y. Savrasov, K. Haule, V. S. Oudovenko, O. Parcollet, and C. A. Marianetti, Rev. Mod. Phys. **78**, 865 (2006).

¹⁶K. Held, Adv. Phys. **56**, 829 (2007).

¹⁷D. Jacob, K. Haule, and G. Kotliar, Phys. Rev. B **82**, 195115 (2010).

¹⁸M. Karolak, T. O. Wehling, F. Lechermann, and A. I. Lichtenstein, J. Phys.: Condens. Matter **23**, 085601 (2011).

¹⁹C. Weber, D. J. Cole, D. D. O’Regan, and M. C. Payne, Proc. Nat. Acad. Sci. **111**, 5790 (2014).

²⁰N. Zaki, H. Park, R. M. Osgood, A. J. Millis, and C. A. Marianetti, Phys. Rev. B **89**, 205427 (2014).

²¹W. Huang, D.-H. Xing, J.-B. Lu, B. Long, W. H. E. Schwarz, and J. Li, J. Chem. Theory Comput. **12**, 1525 (2016).

²²O. Gunnarsson and K. Schönhammer, Phys. Rev. Lett. **56**, 1968 (1986).

²³K. Schönhammer, O. Gunnarsson, and R. M. Noack, Phys. Rev. B **52**, 2504 (1995).

²⁴N. A. Lima, M. F. Silva, L. N. Oliveira, and K. Capelle, Phys. Rev. Lett. **90**, 146402 (2003).

²⁵D. Carrascal, J. Ferrer, J. C. Smith, and K. Burke, J. Phys.: Condens. Matter **27**, 393001 (2015).

²⁶S. Kurth and G. Stefanucci, J. Phys.: Condens. Matter **29**, 413002 (2017).

²⁷N. Sobrino, S. Kurth, and D. Jacob, Phys. Rev. B **102**, 035159 (2020).

²⁸G. Stefanucci and S. Kurth, Phys. Rev. Lett. **107**, 216401 (2011).

²⁹J. P. Bergfield, Z.-F. Liu, K. Burke, and C. A. Stafford, Phys. Rev. Lett. **108**, 066801 (2012).

³⁰P. Tröster, P. Schmitteckert, and F. Evers, Phys. Rev. B **85**, 115409 (2012).

³¹D. Karlsson, A. Privitera, and C. Verdozzi, Phys. Rev. Lett. **106**, 116401 (2011).

³²G. Stefanucci and S. Kurth, Nano Lett. **15**, 8020 (2015).

³³S. Kurth and G. Stefanucci, Phys. Rev. B **94**, 241103(R) (2016).

³⁴D. Jacob and S. Kurth, Nano Lett. **18**, 2086 (2018).

³⁵N. Sobrino, R. D’Agosta, and S. Kurth, Phys. Rev. B **100**, 195142 (2019).

³⁶D. Jacob, G. Stefanucci, and S. Kurth, Phys. Rev. Lett. **125**, 216401 (2020).

³⁷N. Mermin, Phys. Rev. **137**, A1441 (1965).

³⁸J.P. Perdew, R.G. Parr, M. Levy, and J.L. Balduz, Phys. Rev. Lett. **49**, 1691 (1982).

³⁹G. Stefanucci and S. Kurth, Phys. Stat. Sol. (b) **250**, 2378 (2013).

⁴⁰S. Kurth and G. Stefanucci, Phys. Rev. Lett. **111**, 030601 (2013).

⁴¹J. P. Coe, Phys. Rev. B **99**, 165118 (2019).

⁴²J.D. Talman and W.F. Shadwick, Phys. Rev. A **14**, 36 (1976).

⁴³T. Grabo, T. Kreibich, S. Kurth, and E.K.U. Gross, in *Strong Coulomb Correlations in Electronic Structure Calculations: Beyond Local Density Approximations*, edited by V. Anisimov (Gordon and Breach, Amsterdam, 2000), p. 203.

⁴⁴S. Kümmel and L. Kronik, Rev. Mod. Phys. **80**, 3 (2008).

⁴⁵T. Gould and S. Pittalis, Phys. Rev. Lett. **119**, 243001 (2017).

⁴⁶T. Gould and S. Pittalis, Phys. Rev. Lett. **123**, 016401 (2019).

⁴⁷Q. Sun, T. C. Berkelbach, N. S. Blunt, G. H. Booth, S. Guo, Z. Li, J. Liu, J. D. McClain, E. R. Sayfutyarova, S. Sharma, S. Wouters, and G. K.-L. Chan, Wiley Interdiscip. Rev. Comput. Mol. Sci. **8**, e1340 (2018).

⁴⁸A. Szabo and N. S. Ostlund, *Modern Quantum Chemistry* (McGraw-Hill, New York, 1989).

⁴⁹J.P. Perdew, K. Burke, and M. Ernzerhof, Phys. Rev. Lett. **77**, 3865 (1996); *ibid.* **78**, 1396 (1997)(E).

⁵⁰J. Nafziger and A. Wasserman, J. Chem. Phys. **143**, 234105 (2015).

⁵¹Y. Shi, Y. Shi, and A. Wasserman, arXiv:2305.13545 (2023).